

AD-752 543

IMAGING IN CLEAR OCEAN WATER

Harold T. Yura

Aerospace Corporation

Prepared for:

Air Force Systems Command

30 November 1972

DISTRIBUTED BY:

NTIS

National Technical Information Service
U. S. DEPARTMENT OF COMMERCE
5285 Port Royal Road, Springfield Va. 22151

AD752543

Imaging in Clear Ocean Water

Prepared by H. T. YURA
Electronics Research Laboratory

72 NOV 30

Laboratory Operations
THE AEROSPACE CORPORATION

Prepared for SPACE AND MISSILE SYSTEMS ORGANIZATION
AIR FORCE SYSTEMS COMMAND
LOS ANGELES AIR FORCE STATION
Los Angeles, California

Reproduced by
NATIONAL TECHNICAL
INFORMATION SERVICE
U.S. Department of Commerce
Washington, DC 20540

APPROVED FOR PUBLIC RELEASE:
DISTRIBUTION UNLIMITED

DDC
RECEIVED
DEC 12 1972
RECEIVED
B

UNCLASSIFIED
Security Classification

DOCUMENT CONTROL DATA - R & D		
(Security classification of title, body of abstract and indexing annotation must be entered when the overall report is classified)		
1 ORIGINATING ACTIVITY (Corporate author)		2a REPORT SECURITY CLASSIFICATION
The Aerospace Corporation El Segundo, California		Unclassified
		2b GROUP
3. REPORT TITLE		
IMAGING IN CLEAR OCEAN WATER		
4 DESCRIPTIVE NOTES (Type of report and inclusive dates)		
5 AUTHOR(S) (First name, middle initial, last name)		
Harold T. Yura		
6 REPORT DATE	7a TOTAL NO. OF PAGES	7b NO OF REFS
72 NOV 30	20	8
8a CONTRACT OR GRANT NO.	9a ORIGINATOR'S REPORT NUMBER(S)	
F04701-72-C-0073	TR-0073(9230-10)-2	
b PROJECT NO.		
c	9b OTHER REPORT NO(S) (Any other numbers that may be assigned this report)	
d	SAMSO-TR-72-268	
10 DISTRIBUTION STATEMENT		
Approved for public release and sale; distribution unlimited.		
11 SUPPLEMENTARY NOTES	12. SPONSORING MILITARY ACTIVITY	
	Space and Missile Systems Organization Air Force Systems Command Los Angeles Air Force Station	
13 ABSTRACT		
<p>A parametric analysis is given of imaging in backscattered light in clear ocean water characterized by temperature and salinity inhomogeneities whose scale length is large compared to the diameter of the light beam. An expression for the beam pattern of a finite underwater laser beam is derived where the effects of source coherence on the imaging properties of backscattered light are discussed. On the basis of the model assumed here, it is concluded that the resolution cannot be significantly improved by reduction of the camera threshold. This limitation results from the rapid decrease of the modulation transfer function for increasing spatial frequencies, which indicates that image modulation below two percent falls another 10 dB at only negligibly higher spatial frequencies. Thus, a 10-dB improvement in the limiting resolution of the camera will not result in significantly better image quality through ocean water.</p> <p>ia</p>		

UNCLASSIFIED

Security Classification

14

KEY WORDS

Imaging
Inhomogeneous media
Lasers
Underwater propagation

Distribution Statement (Continued)

Abstract (Continued)

UNCLASSIFIED
Security Classification

Air Force Report No.
SAMSO-TR-72-268

Aerospace Report No.
TR-0073(9230-10)-2

IMAGING IN CLEAR OCEAN WATER

Prepared by
H. T. Yura
Electronics Research Laboratory

72 NOV 30

Laboratory Operations
THE AEROSPACE CORPORATION

Prepared for
SPACE AND MISSILE SYSTEMS ORGANIZATION
AIR FORCE SYSTEMS COMMAND
LOS ANGELES AIR FORCE STATION
Los Angeles, California

Approved for public release and sale;
distribution unlimited.

10

FOREWORD

This report is published by The Aerospace Corporation, El Segundo, California, under Air Force Contract No. F04701-72-C-0075.

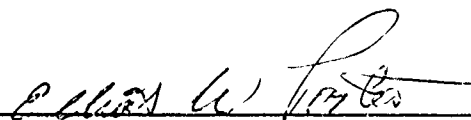
This report, which documents research carried out from May 1972 to July 1972, was submitted on 9 October 1972 to Lt Col Elliott W. Porter, DYA, for review and approval.

Approved



A. H. Silver, Director
Electronics Research Laboratory

Publication of this report does not constitute Air Force approval of the report's findings or conclusions. It is published only for the exchange and stimulation of ideas.



ELLIOTT W. PORTER, LtCol, USAF
Asst Director, Development Directorate
Deputy for Technology

ABSTRACT

A parametric analysis is given of imaging in backscattered light in clear ocean water characterized by temperature and salinity inhomogeneities whose scale length is large compared to the diameter of the light beam. An expression for the beam pattern of a finite underwater laser beam is derived where the effects of source coherence on the imaging properties of backscattered light are discussed. On the basis of the model assumed here, it is concluded that the resolution cannot be significantly improved by reduction of the camera threshold. This limitation results from the rapid decrease of the modulation transfer function for increasing spatial frequencies, which indicates that image modulation below two percent falls another 10 dB at only negligibly higher spatial frequencies. Thus, a 10-dB improvement in the limiting resolution of the camera will not result in significantly better image quality through ocean water.

CONTENTS

FOREWORD	ii
ABSTRACT	iii
I. INTRODUCTION	1
II. COHERENCE EFFECTS	3
A. Parametric Analysis of Visibility in Clear Ocean Water	3
B. Beam Patterns	9
C. Limiting Resolution	15
FOOTNOTES	17
APPENDIX. EVALUATION OF AN INTEGRAL	19

FIGURES

1. Spherical-Wave MTF as Function of Transverse Separation ρ and Spatial Frequency f for Various Values of R and $\langle \Delta n^2 \rangle$	6
2. Schematic Diagram of Underwater Laser Propagation	8
3. Normalized Intensity $I_N(\theta)$ as Function of θ for $a = 50$ cm and Various Values of R	12
4. Angle θ_0 as Function of R for Various Values of a	13

Preceding page blank

I. INTRODUCTION

The imaging properties of collimated laser beams propagating through ocean water have recently attracted considerable attention. Direct or indirect viewing is necessary to carry out such underwater activities as target acquisition, guidance of submarines, and the search for metal nodules or marine specimens. Clear ocean water (i.e., free of particulate matter) is inhomogeneous because of the existence of random variations in salinity and temperature. Both quantities affect the index of refraction of water; consequently, a laser beam employed to illuminate a subsurface object, even in clear ocean water, may be subject to severe degradation. Whether a laser beam is to be used for ranging or illumination (in direct or in TV viewing) or for communication, knowledge of its behavior is essential. The complex interrelationships among natural limitations and the necessity of obtaining a clear image impose severe restrictions on designers of underwater equipment that employ coherent light beams. In this paper, mathematical expressions are presented that permit estimation of the performance of proposed equipment in clear ocean water under various operational conditions.

In particular, this paper presents a parametric analysis of underwater imaging in backscattered light in ocean waters that are relatively free of particulate matter. In this case, light is scattered by refractive-index variations in the water resulting from large-scale (some tens of centimeters) thermal and saline variations (about their respective means). Ocean waters of this type, which have long attenuation lengths (≥ 8 m) in the blue-green region of the spectrum, occur in several geographical locations:^{1,2} e.g., the Caribbean Sea, the Pacific North Equatorial Current, the Pacific Countercurrent, the Pacific Equatorial Divergence, the Pacific South Equatorial Current, and the Sargasso Sea.

The mutual-coherence function, defined as the cross-correlation function of the complex field in a direction transverse to the direction of propagation, describes the loss of coherence of an initially coherent wave propagating

in an inhomogeneous medium. It follows that the mutual-coherence function is important for a number of practical applications. It determines the limiting resolution obtainable in forming an image through an inhomogeneous medium, the mean intensity distribution from an initially coherent wave emanating from a finite transmitting aperture, the limiting holographic resolution in an inhomogeneous medium, and the signal-to-noise ratio in a heterodyne detection system.

Section II presents a parametric analysis of visibility in clear ocean water. The effects of source coherence on the imaging properties of back-scattered light are discussed. In addition, an expression for the beam pattern of an underwater laser beam is presented, and the quantitative relationships of image resolution, beam spread, and temperature and salinity fluctuations are discussed. Finally, an expression for the limiting resolution in clear ocean water is presented.

II. COHERENCE EFFECTS

A. PARAMETRIC ANALYSIS OF VISIBILITY IN CLEAR OCEAN WATER

This paper treats time-averaged quantities in which, for a homogeneous isotropic turbulent medium, the mutual coherence function is real; this function is referred to here as the modulation transfer function (MTF). Furthermore, we invoke the ergodic hypothesis, in which the time average and the ensemble average are assumed equal. The calculations that follow pertain to the case of large-scale (in comparison with laser beam diameter) thermal and saline variations about their respective means.

Yura³ has given a quantitative analysis of small-angle ($\lesssim 1$ mrad) scattering of light in ocean water by suspended biological particles with an index of refraction close to that of water and large-scale (in comparison with the laser-beam diameter, $\lesssim 1$ cm) index-of-refraction variations due to thermal and saline inhomogeneities. In particular, he has calculated, for plane waves, the MTF for these two scattering mechanisms and has shown that (for values of the transverse distance ρ less than the size of the large-scale index-of-refraction fluctuations but larger than the size of the suspended biological particles) the MTF's due to the two mechanisms have different functional dependences on transverse distance. In particular, for the case of large-scale index-of-refraction variations, he finds that³

$$M(\rho, R) = \exp \left[- \frac{k^2 \rho^2 \langle \Delta n^2 \rangle R}{4a} \right] \quad (1)$$

where $\langle \Delta n^2 \rangle$ is the rms index-of-refraction variation, a is the characteristic scale length of the inhomogeneity (assumed greater than the laser beam diameter), ρ is the transverse distance at propagation distance R , k is the optical wave number ($2\pi n/\lambda$), and angular brackets denote the ensemble average.

For calculation of such quantities as resolution and beam spreading, the MTF of a point source (i.e., spherical wave) must be known. In this case, the spherical-wave MTF is obtained from the plane-wave MTF by replacement of ρ^2 by $\int_0^1 (\rho u)^2 du$, which equals $\rho^2/3$.⁴

$$M_S(\rho, R) = \exp \left(- \frac{\rho^2 k^2 \langle \Delta n^2 \rangle R}{12a} \right) \quad (2)$$

The mean-square index variation $\langle \Delta n^2 \rangle$ is given by

$$\langle \Delta n^2 \rangle = \left(\frac{\partial n}{\partial T} \right)^2 \langle \Delta T^2 \rangle + \left(\frac{\partial n}{\partial S} \right)^2 \langle \Delta S^2 \rangle \quad (3)$$

where $\langle \Delta T^2 \rangle$ and $\langle \Delta S^2 \rangle$ are the mean-square temperature and salinity variations (about their respective means). In deriving Eq. (3), we have assumed that, to a first approximation, temperature and salinity are independent random variables. Typically, $\langle \Delta T^2 \rangle^{1/2}$ is a few hundredths to a few tenths of a degree, absolute;⁵ however, no data are readily available on $\langle \Delta S^2 \rangle$. Also, the characteristic scale length a for temperature fluctuations is on the order of tens of centimeters.⁵

In general, the incremental index-of-refraction variation Δn is related to the incremental density variation Δd by

$$\Delta n = \left(\frac{\Delta d}{d} \right) \left(\frac{n^2 - 1}{2n} \right) \left(\frac{n^2 + 2}{3} \right) \quad (4)$$

where d is the density ($=1.02 \text{ g/cm}^3$ for ocean water). In deriving Eq. (4), we have neglected the change of polarizability of the constituent molecules with changes in density. For the values of the relative temperature and salinity variations considered here, order-of-magnitude estimates of the resulting change in the polarizability show that this neglect is justified. Assuming that temperature and salinity variations are independent variables, we may write $\Delta d = (\Delta d)_T + (\Delta d)_S$, where

$$\left(\frac{\Delta d}{d}\right)_T = -\alpha \Delta T \quad (5)$$

where α is the coefficient of volume expansion ($\sim 2.1 \times 10^{-4}/^\circ\text{C}$ for water in the range 0 to 33°C), and $(\Delta d)_S = \Delta(d_S)$, where d_S is the saline contribution to the density (i.e., the concentration of the salt times its density). Hence, on squaring and taking an ensemble average, we obtain

$$\langle \Delta n^2 \rangle = \left(\frac{n^2 - 1}{2n}\right)^2 \left(\frac{n^2 + 2}{3}\right)^2 \left\{ \left[\alpha^2 \langle \Delta T^2 \rangle \right] + [\Delta d_S]^2 \right\} \quad (6)$$

Since no data are readily available on Δd_S , we consider temperature variations only in the following. In this case we find that, for ocean water ($n \approx 1.34$),

$$\langle \Delta n^2 \rangle \approx 0.6 \times 10^{-8} \langle \Delta T^2 \rangle \quad (7)$$

For example, for $10^{-10} < \langle \Delta n^2 \rangle < 10^{-9}$, we find from Eq. (7) that $0.13^\circ\text{C} < \langle \Delta T^2 \rangle^{1/2} < 0.41^\circ\text{C}$. (Since saline variations have been neglected, these rms temperature variations are to be regarded as an upper limit.)

Figure 1 is a graph of the spherical wave MTF [i.e., Eq. (2)] for $\lambda = 0.5 \mu\text{m}$ over the range of interest. The upper abscissa is given for ρ in centimeters, while the lower one is given for spatial frequency f in cycles/milliradian ($f = \rho/2\lambda$). Values of the parameters $\langle \Delta n^2 \rangle$ and scale length a were chosen for which the MTF would be about 2 percent at about 1.0 to 10.0 cycles/mrad and $\lambda = 0.5 \mu\text{m}$, with the constraint that the scale length a have a reasonable value. The curves are shown for $a = 50 \text{ cm}$ and $\langle \Delta n^2 \rangle = 10^{-10}$ and 10^{-9} .

Receiving systems differ greatly in their resolution thresholds. Furthermore, these thresholds are a function of contrast⁶ and level of illumination reaching the receiver.⁷ However, even a few tenths of a watt of laser illumination should be adequate to realize the limiting resolution of current low-level television systems. For any given receiving system there is some

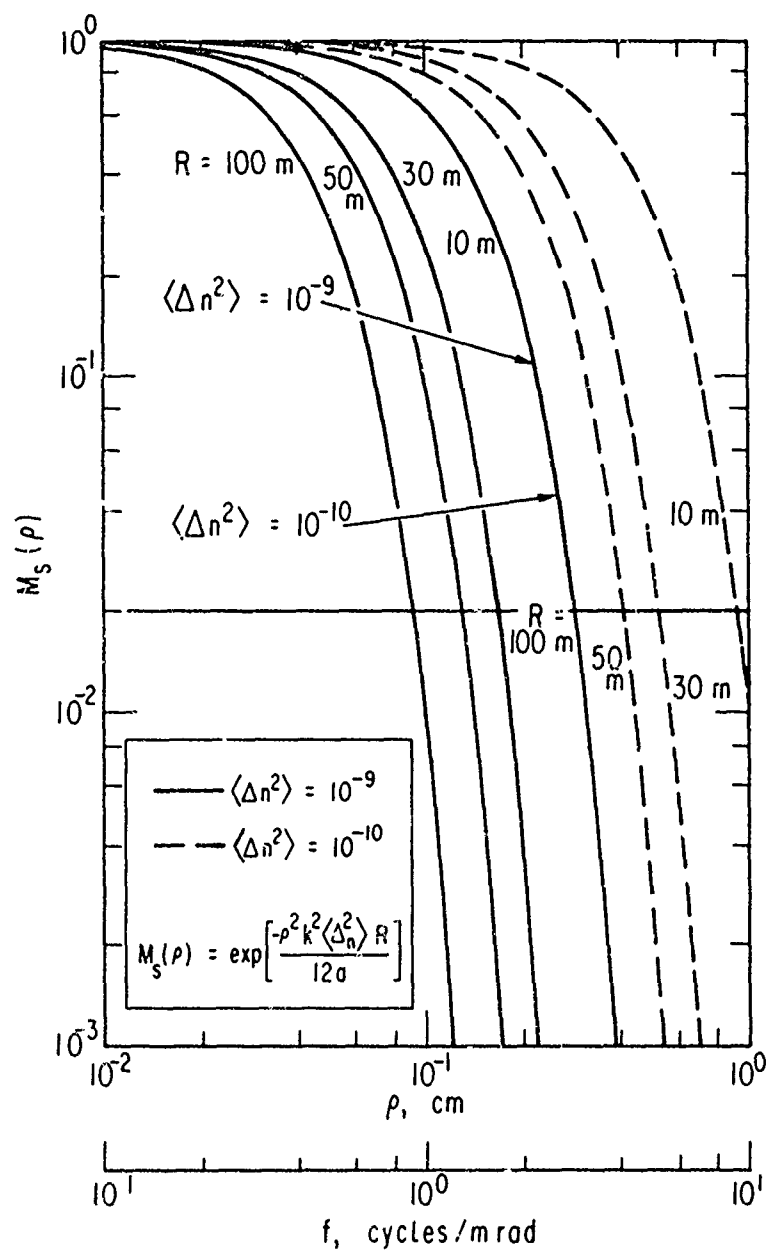


Figure 1. Spherical-Wave MTF as Function of Transverse Separation ρ and Spatial Frequency f for Various Values of R and $\langle \Delta n^2 \rangle$

number m_0 (<1) for which, if the MTF is less than m_0 , resolution is not possible. Defining ρ_{\max} so that, for a fixed propagation distance R , $M(\rho \leq \rho_{\max}) \leq m_0$, we note that the minimum distance resolvable in the object plane Δx_{\min} is related to the maximum transverse distance in the receiving aperture ρ_{\max} (assuming $\rho_{\max} < \text{receiver diameter}$) by

$$\Delta x_{\min} \approx \frac{R}{k\rho_{\max}} \quad (8)$$

The contrast degradation caused by the medium is described by Fig. 1, in which the 2-percent modulation level⁷ is marked by the heavy horizontal line. From Fig. 1 we see that, for the case of large-scale index variations, $M \geq 2$ percent for $0.1 < \rho < 1.0$ cm.

In general, to determine the effective resolution through such a medium, one should plot the limiting resolution as a function of apparent contrast for the receiver of interest. The intersection between the limiting resolution curve of the camera and the MTF of the medium is the achievable resolution. For example, at 7-percent contrast (about 3.5-percent modulation) and high light levels, the limiting resolution for a 1-in. image orthicon, S-10 photocathode, $f/1.5$ optics, 6-Mc gain bandwidth, is about 16 TV lines/mm.^{8,9} With a 1-m focal length, this corresponds to a spatial frequency of 8 cycles/mrad. But from Fig. 1 we see that, except for $\langle \Delta n^2 \rangle = 10^{-10}$ at a range of 10 m, the medium has degraded the apparent contrast of a high-contrast (i.e., 100-percent modulation) object much below 7 percent (3.5-percent modulation) at 8 cycles/mrad. We do not have data on camera performance at very low contrast, but one might extrapolate that at high light levels one could resolve a few cycles/mrad at 2-percent image modulation. This threshold level is indicated in Fig. 1.

It is important to note that imaging systems have a limiting resolution, even at high light levels. It follows that increasing the illumination indefinitely does not continue to improve the resolution.

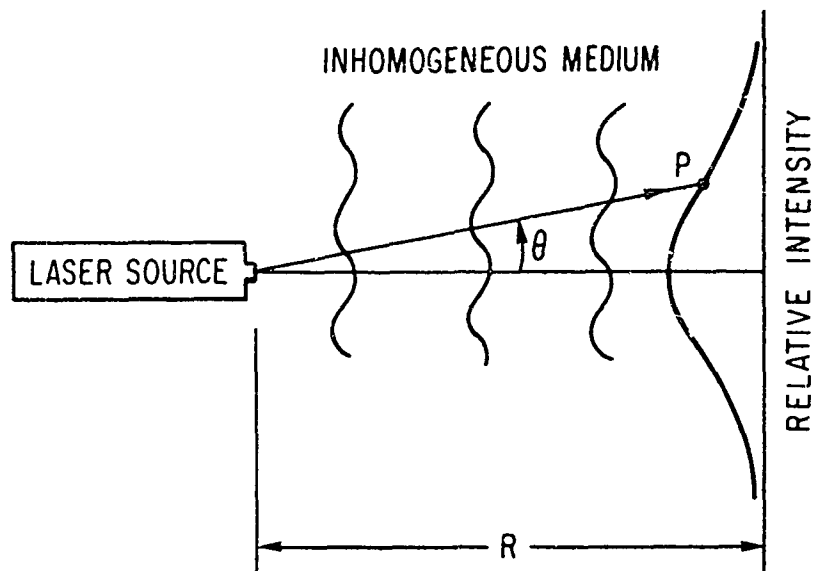


Figure 2. Schematic Diagram of Underwater Laser Propagation

Finally, if the MTF of the medium is indeed as shown in Fig. 1, resolution cannot be significantly improved by reduction of the camera threshold. This limitation is a result of the steep drop of the MTF shown in Fig. 1, which indicates that the image modulation below 2 percent falls another 10 dB at only negligibly higher spatial frequencies. Thus a 10-dB improvement in the limiting resolution of the camera will not result in significantly better image quality through these waters.

The inherent resolution of the receiver is attained when the wavefront from each resolvable element of the object has transverse coherence and uniform phase and amplitude across the whole receiver aperture. The coherence of the radiation illuminating the object is important only in the formation of holograms or for the special case of observation of a specular object. For incoherent imaging (e.g., photography and television), on the other hand, coherent illumination will result in interference effects (e.g., speckle pattern) that can degrade the image. Such effects will be observed if the wavefront reaching the object exhibits coherence over separations greater than that corresponding to the size of a resolvable element in the receiver. The intensity of the illumination at the object is a function of the collimation or focusing of the beam; in either case the intensity is maximum when the source exhibits transverse coherence over separations equal to its exit aperture.

If the medium dominates, the dimensions of the region of the object coherently illuminated may be taken as the e^{-1} point of the MTF curves in Fig. 1. For the parameters plotted, these values are between 0.05 and 0.5 cm (using the upper scale of the abscissa). In order that interference phenomena not introduce additional noise, the angular resolution of the receiver should be greater than this value at the object. At 20 m range this corresponds to an angle between 3×10^{-5} and 3×10^{-4} rad.

B. BEAM PATTERNS

Another quantity of interest is the average spatial intensity distribution as a function of θ , where the angle θ is indicated in Fig. 2.

The average intensity at observation point P of a laser beam described by an aperture function $U(\underline{r})$ in the plane $R = 0$ is given by

$$\begin{aligned} \langle I(\underline{P}) \rangle = & e^{-\alpha R} \left(\frac{1}{R\lambda} \right)^2 \int d^2 \underline{\rho} M_S(\underline{\rho}, R) e^{-(ik/R)\underline{P} \cdot \underline{\rho}} \\ & \times \int U(\underline{r} + \frac{1}{2}\underline{\rho}) U^*(\underline{r} - \frac{1}{2}\underline{\rho}) e^{(ik/R)\underline{\rho} \cdot \underline{r}} d^2 \underline{r} \end{aligned} \quad (9)$$

(The quantity α in Eq. (9) is the spectral volume attenuation coefficient [the sum of the volume absorption coefficient and the volume scattering ($\geq 10^{-2}$ rad) coefficient]. The effect of these absorptions and scatterings at range R is taken into account in expressions involving the square of the field by the factor $\exp(-\alpha R)$. This factor is to be understood and is omitted in the following. The large-angle scattering and absorption result in a loss of power from the beam. There is no way of distinguishing between absorption and large-angle scattering ($> 10^{-2}$ rad) by measuring optical properties in the forward direction.) As an example, consider a plane wave of uniform amplitude and phase emanating from a circular aperture of diameter D ; Eq. (9) becomes

$$\langle I(P) \rangle = \frac{8}{\pi} \beta^2 \int_0^1 x J_0(2\alpha x) M_S(Dx, R) \Gamma_\beta(x) dx \quad (10)$$

where M_S is the spherical-wave MTF for the medium, $x = \rho/D$, $\beta = kD^2/4R$, and

$$\Gamma_\beta(x) = \int_0^{\cos^{-1}(x)} d\theta \left[\frac{\sin[2\beta x(\cos \theta - x)]}{(2\beta x \cos \theta)} - \frac{\{1 - \cos[2\beta x(\cos \theta - x)]\}}{(2\beta x \cos \theta)^2} \right]$$

for $x \leq 1$

$$= 0 \text{ for } x > 1 \quad (11)$$

J_0 is the zero-order Bessel function, and $\alpha = kD\rho/2R = kD \tan \theta/2 \approx kD\theta/2$, since $\theta \ll 1$. Normalizing the intensity at a fixed range R to the value on the axis ($\theta = 0$), we obtain

$$\langle I_N(\theta) \rangle = \frac{\int_0^1 x J_0(2\alpha x) M_S(Dx, R) \Gamma_\beta(x) dx}{\int_0^1 x \Gamma_\beta(x) M_S(Dx, R) dx} \quad (12)$$

The Fresnel and Fraunhofer regions are for values of β greater than or less than one, respectively. We note that for $\lambda \approx 0.5 \mu\text{m}$, $D = 2 \text{ cm}$ and $R \leq 100 \text{ m}$, $\beta \geq 17$. That is, for all cases of interest we are in the Fresnel region of the transmitting aperture.

The spherical wave MTF is given by Eq. (2). Substituting this into Eq. (10) yields (see Appendix)

$$\langle I_N(\theta) \rangle \approx \exp(-\theta^2/2\theta_0^2) \quad (13)$$

where

$$\theta_0^2 = \frac{\langle \Delta n^2 \rangle R}{6a} \quad (14)$$

In Fig. 3 we plot the normalized intensity I_N as a function of θ for $a = 50 \text{ cm}$ and various values of R and $\langle \Delta n^2 \rangle$. The quantity θ_0 is the angle corresponding to the standard deviation of the gaussian beam pattern and is of the order of few tenths of a milliradian, it is plotted in Fig. 4 for various values of $\langle \Delta n^2 \rangle$ and a . The curves presented here indicate the values of beam spread one would expect to observe when imaging resolution of a few tenths of a milliradian is achieved. On the other hand, the half-power cone angle in the absence of index-of-refraction fluctuations is of the order λ/D , i.e., a few times 10^{-2} mrad for $\lambda \sim 5 \times 10^{-5} \text{ cm}$ and D of some centimeters. Hence, for R of some tens of meters and $\langle \Delta n^2 \rangle \geq 10^{-9}$, the beam is spread by one order of magnitude by the large-scale index-of-refraction fluctuations.

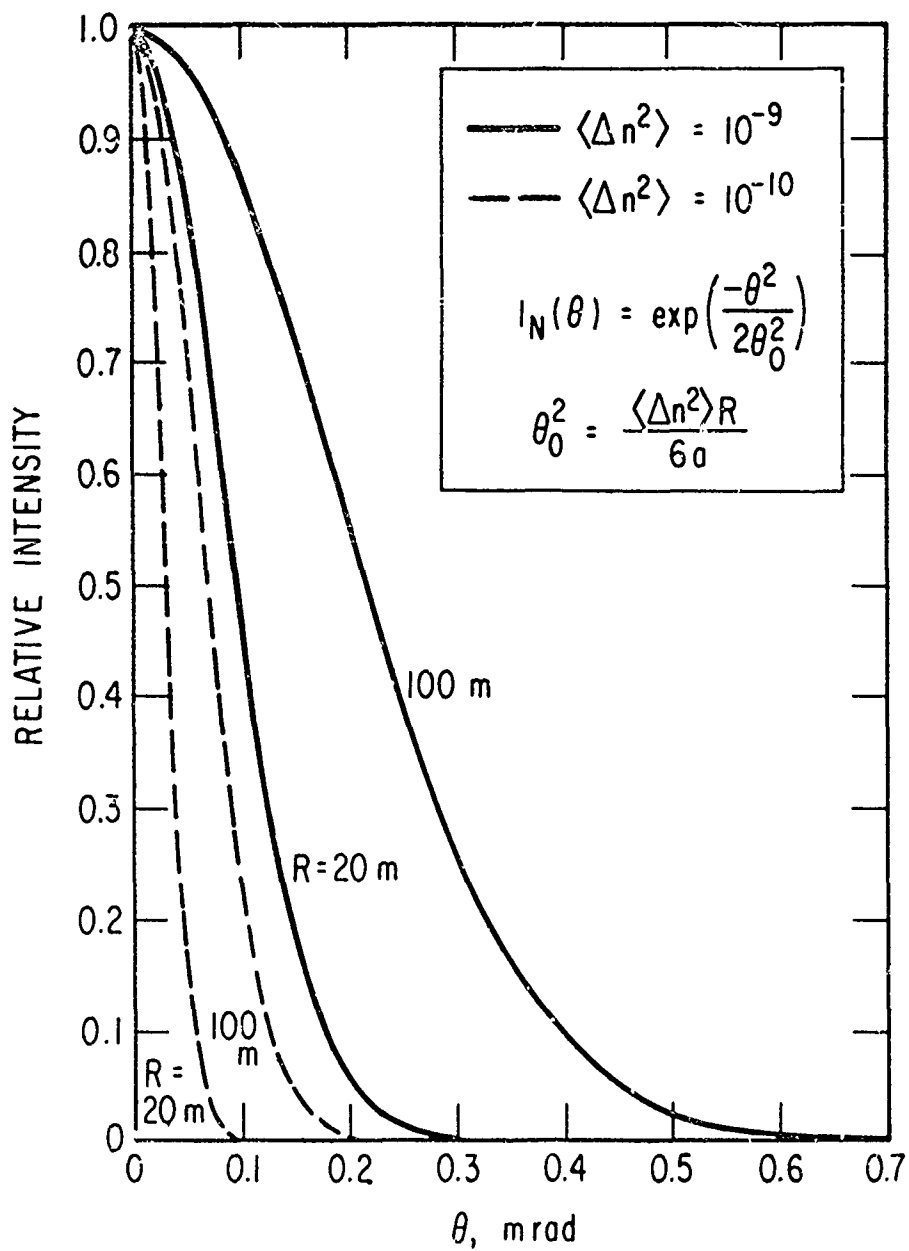


Figure 3. Normalized Intensity $I_N(\theta)$ as Function of θ for $a = 50$ cm and Various Values of R

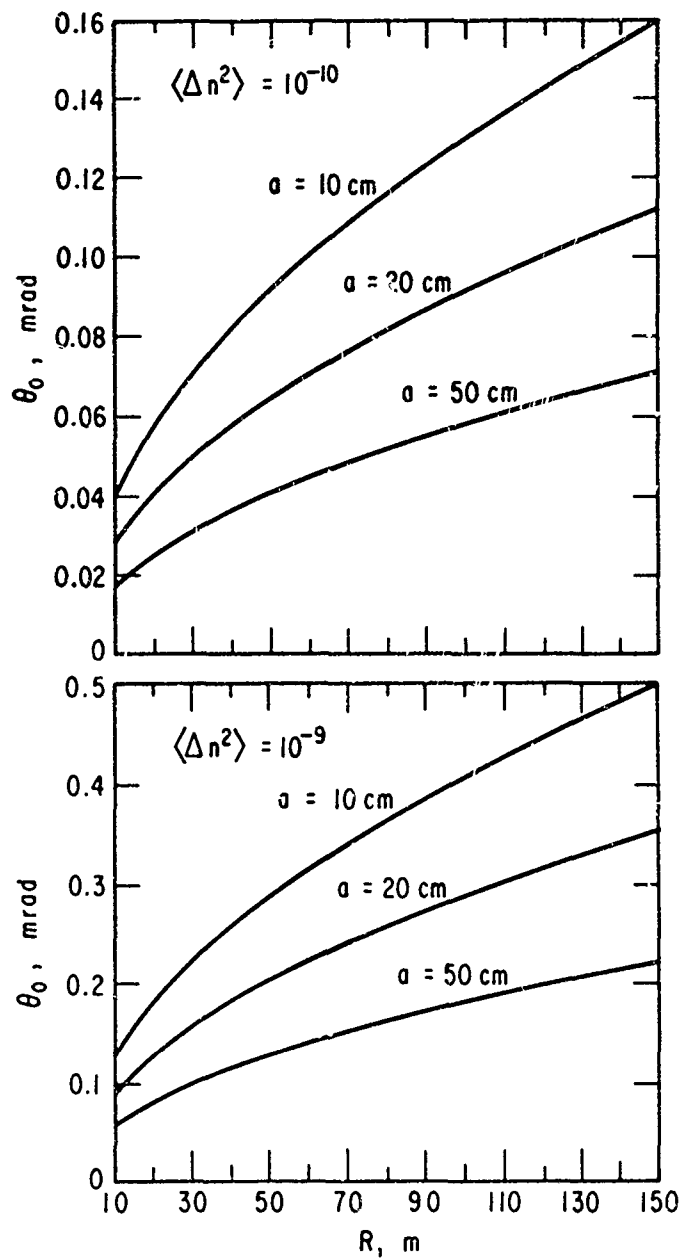


Figure 4. Angle θ_0 as Function of R for Various Values of a

(θ_0 corresponds to the standard deviation of the Gaussian beam pattern.)

From Fig. 3, we note that if propagation were determined by large-scale temperature and salinity fluctuations of the magnitude assumed and if the source were perfectly coherent, the half-power beam width even at a range of 20 m would lie between 0.06 and 0.2 mrad. This corresponds to a coherent radiator in vacuum of between 0.3- and 0.9-cm diam. Therefore, for work at 20 m, there appears to be no need for greater transverse coherence, and at greater ranges the requirement is reduced still further.

As a possible experimental method of measuring the MTF, we note that Eq. (10) is merely the Fourier-Bessel transform of the quantity $\beta^2 M_S(Dx, R) \Gamma_\beta(x)$, which can be inverted to yield¹¹

$$D^2 \Gamma_\beta(\rho/D) M_S(\rho, R) = 2\pi \int_0^\infty J_0\left(\frac{k\rho}{R} p\right) \langle I(\rho, R) \rangle p \, dp \quad (15)$$

Hence, if the relative intensity $\langle I \rangle$ is known experimentally (say, from a microdensitometer technique applied to a direct exposure of a photographic plate to the laser beam at range R), one obtains directly the quantity M_S [by numerically integrating the righthand side of Eq. (15)]. The quantity $\Gamma_\beta(\rho/D)$ is essentially the MTF of the transmitting aperture and is assumed known (or can be measured directly).

The MTF obtained by integration of Eq. (15) can be compared to the theoretical expression

$$M_S(\rho, R) = \exp\left(-\frac{\rho^2 k^2 \langle \Delta n^2 \rangle R}{12a}\right)$$

if the quantities a and $\langle \Delta n^2 \rangle$ are measured simultaneously with $\langle I(\theta) \rangle$. We remark that, with θ_0 defined by Eq. (14), the MTF can be written as

$$M_S(\rho, R) = \exp\left(-\frac{\rho^2 k^2 \theta_0^2}{2}\right)$$

Therefore, a measurement of the angle θ_0 , where the relative intensity is down by $1/\sqrt{e}$ in comparison with its on-axis value), results in a determination of the MTF. The MTF so obtained can then be compared with other simultaneous measurements of the MTF. Consequently, these functions, M_S and $\langle I \rangle$, provide a means of tying together independent measurements of resolution, beam divergence, and temperature and salinity fluctuations.

C. LIMITING RESOLUTION

In conclusion we present an expression for the limiting resolution in clear ocean water. The imaging properties of the water are described by the MTF. In the model suggested here, the MTF is given by Eq. (2). The transverse distance ρ in this expression is related to the spatial frequency f by

$$f = \frac{\rho}{2\lambda} \text{ (cycles/rad)}$$

and the corresponding angular resolution δ by

$$\delta = \frac{2}{f} = \frac{\lambda}{\rho}$$

From Eq. (2) we can find the value of ρ corresponding to the threshold of modulation m_0 for some camera

$$\rho_0 = \left(\frac{\ln m_0}{\eta k^2 R} \right)^{1/2}$$

where $\eta = \langle \Delta n^2 \rangle / 12a$, and therefore the limiting angular resolution is

$$\delta_0 = 2\pi \left(\frac{\eta R}{\ln m_0} \right)^{1/2} \quad (16)$$

Consequently, the limiting resolution is independent of wavelength.

FOOTNOTES

1. S. J. Duntley, J. Opt. Soc. Am. 53, 214 (1963).
2. N. G. Jerlov, Optical Oceanography (Elsevier Publishing Co., New York, 1968).
3. H. T. Yura, Appl. Opt. 10, 114 (1971).
4. R. F. Lutomirski and H. T. Yura, J. Opt. Soc. Am. 61, 482 (1971).
5. L. Lieberman, J. Acoust. Soc. Am. 23, 563 (1951).
6. For example, the minimum useful contrast of photographic film is a function of spatial frequency and is about 2 percent at 50 cycles/mm.
7. Modulation $m = C/(2 + C)$, where the contrast $C = (\text{highlight} - \text{lowlight} / \text{lowlight})$.
8. H. V. Söule, Electro-Optical Photography at Low Illumination Levels (John Wiley and Sons, Inc., New York, 1968), p. 129.
9. F. A. Rosell, J. Opt. Soc. Am. 59, 539 (1969).
10. R. F. Lutomirski and H. T. Yura, Appl. Opt. 10, 1652 (1971).
11. Note that Eq. (10) holds only for a uniform disturbance over a circular aperture of diameter D .

Preceding page blank

APPENDIX. EVALUATION OF AN INTEGRAL

We wish to compute

$$I = \int_0^1 x J_0(2\alpha x) M_S(Dx, R) \Gamma_\beta(x) dx \quad (A-1)$$

where Γ_β is given by Eq. (11) and

$$M_S(Dx, R) = \exp\left(-\frac{D^2 x^2 k^2 \langle \Delta n^2 \rangle R}{12a}\right) \quad (A-2)$$

Substituting Eq. (A-2) into Eq. (A-1), we obtain

$$I = \int_0^1 x J_0(2\alpha x) \Gamma_\beta(x) \exp(-\alpha^2 x^2) dx \quad (A-3)$$

where

$$\gamma^2 = k^2 D^2 R \langle \Delta n^2 \rangle / 12a$$

For all cases of interest, $\gamma \gg 1$ (for $k \sim 10^5 \text{ cm}^{-1}$, $D = 2 \text{ cm}$, $R = 100 \text{ m}$, $a \simeq 50 \text{ cm}$, and $\langle \Delta n^2 \rangle \sim 10^{-9}$, $\gamma \sim 10^5$). Let $y = \gamma x$; then

$$I = \gamma^{-2} \int_0^\gamma y J_0\left(\frac{2\alpha}{\gamma} y\right) \exp(-y^2) \Gamma_\beta(y/\gamma) dy$$

Preceding page blank

The integrand is nonzero only for y less than of the order unity. Since $\gamma \gg 1$, we may replace the upper limit of the integral by ∞ and substitute $\Gamma_\beta(0) (= \pi/4)$ for $\Gamma_\beta(y/\gamma)$. We obtain

$$\begin{aligned} I &\simeq \frac{\pi}{4\gamma^2} \int_0^\infty y J_0\left(\frac{2\alpha}{\gamma} y\right) \exp(-y^2) dy \\ &= \frac{\pi}{8\gamma^2} \exp(-\alpha^2/\gamma^2) \end{aligned}$$